SHEAR-FRICTION STRENGTH OF REINFORCED CONCRETE STRUCTURAL WALLS

Saman Ali Abdullah, PhD[1]

[1] Lecturer, University of Sulaimani, Kurdistan Region, Iraq. (E-mail: eng.saman86@gmail.com)

Abstract: *Most of the provisions for concrete structural walls in ACI 369.1-17 were developed in the late 1990s based on limited experimental data and judgement for FEMA-273 (1997a) and FEMA-274 (1997b). The only exception being the modeling parameters and acceptance criteria of shear-controlled walls, which were updated for the ASCE/SEI 41-06 Supplement 1. As a result, the wall provisions tend to be, in many cases, inaccurate and conservative. Currently, shear-friction-controlled walls are currently treated as force-controlled components (actions), which is overly conservative since shear-friction mechanism in walls tends to be a relatively ductile action and thus can produce uneconomical retrofit schemes. This is primarily due to lack of experimental data to develop appropriate provisions for these walls. To address this issue, this study involves utilizing available experimental data and new information on performance of structural walls to first study various issues related to shear-friction-controlled walls and propose updated modeling parameters and acceptance criteria for shear-friction-controlled walls that will produce improved seismic assessments of wall buildings. Due to limited space, only shear-friction strength related results are presented.*

1 Introduction

The concept of shear-friction strength was originally developed in the 1960s (Birkeland and Birkeland, 1966; Hofbeck et al., 1969) to evaluate shear transfer across a concrete-to-concrete interface crossed by reinforcement perpendicular to the interface. The concept has been further studied over the years (Mattock, 1976 and 1977; Kahn and Mitchell, 2002). These studies indicate that shear-friction (interface) strength results from: (a) cohesion between particles (direct bearing of asperities and aggregate interlock), (2) friction between concrete parts or crack faces (ACI 318 approach), and (3) dowel action of the reinforcement crossing the interface (to a minor extent). ACI 318 first adopted shear-friction provisions in 1971 based on the work of Hofbeck et al. (1969). The ACI 318 approach for shear-friction strength (ACI 318-19 Section 22.9.4), which is given by Eq. 3-1, only considers the contribution of friction between concrete surfaces, where A_{vf} is the area of reinforcement crossing the sliding interface, f_y is the design yield strength of the reinforcement, μ is the coefficient of friction accordance with Table 1 (ACI 318-14 Table 22.9.4.2), and P is the sustained axial load on the sliding interface if present. In ACI 318-19 Table 22.9.4.2, reproduced as Table 1, the interface type significantly impacts shear-friction strength (strength changes by a factor of 2.33). Cold joints that meet ACI 318 roughness definition (1/4 in. amplitudes) are treated as 1.67 times stronger than their “smooth” counterparts. Monolithic interfaces are treated as 2.33 times stronger than their “smooth” counterparts. As shown Table 1, upper-bound limits are applied primarily due the lack of sufficient data when these provisions were adopted.

$$V_n = \mu\left(A_{vf} f_y + P\right) \qquad \text{(Eq. 1)}$$

Table 1. Shear-friction coefficients and strength upper-bounds of ACI 318-19

Interface Type	μ	Maximum shear-friction strength, $V_{n,max}$
Monolithic (concrete to concrete)	1.4λ	For normal-weight concrete (monolithic or roughened): Least of $\begin{Bmatrix} 0.2f'_{cE}A_c \\ (480+0.08f'_{cE})A_c \\ 1600A_c \end{Bmatrix}$ For all other cases: Lesser of $\begin{Bmatrix} 0.2f'_{cE}A_c \\ 800A_c \end{Bmatrix}$
Roughened (concrete to concrete)	1.0 λ	
Concrete placed against hardened concrete not roughened intentionally	0.60 λ	
Concrete anchored to an as-rolled structural still by headed studs or by reinforcing bars	0.70 λ	

Note: f'_c is the design concrete compressive strength, μ is the coefficient of friction, A_c is the area of concrete section resisting shear transfer, and l is the modification factor to reflect the reduced mechanical properties of lightweight concrete relative to normalweight concrete of the same compressive strength.

One of the principal limitations of the ACI 318 approach for shear-friction strength, as it applies to concrete walls, is that this approach was developed and verified using results from “push-off” tests under primarily monotonic loading. Under earthquake loading, wall interfaces are typically subjected to cyclic moments, shears, and axial loads and the contributions of direct bearing of asperities and reinforcement dowel action are likely reduced under these conditions. Mattock (1977) concluded that repeated cyclic loading degrades shear-friction resistance to roughly 80% of monotonic strength.

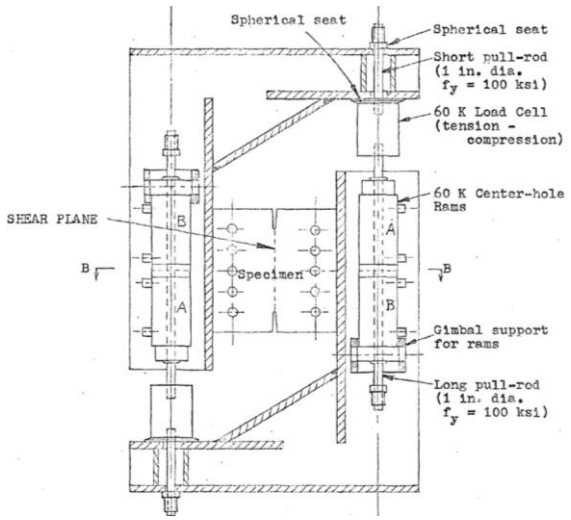

Figure 1. Push-off test setups used to study shear-friction strength (Mattock, 1976; 1977).

The ASCE/SEI 41 standard (and other similar standards or guidelines, e.g., ACI 369 standard) represents a major advance in structural and earthquake engineering to address the seismic hazards posed by existing buildings and mitigate those hazards through retrofit. For nonlinear seismic evaluation of existing buildings, these standards provide modeling parameters (e.g., effective stiffness values, deformation capacities, and strengths) to construct backbone relations, as well as acceptance criteria to determine the adequacy. The modeling parameters and acceptance criteria for structural concrete walls were developed based on limited experimental data and knowledge available in the late 1990s (FEMA 273/274-1997), with minor revisions since. As a result, the wall provisions tend to be, in many cases, inaccurate and conservative. Currently, shear-friction-controlled walls are currently treated as force-controlled components (actions), which is overly conservative since shear-friction mechanism in walls tends to be a relatively ductile action and thus can produce uneconomical retrofit schemes. This is primarily due to lack of experimental data to develop appropriate provisions for these walls. To address this issue, this study involves utilizing available experimental data and new information on performance of structural walls to first study various issues related to shear-friction-controlled walls and propose updated shear-friction strength relations that will produce improved seismic assessments of wall buildings. To accomplish these objectives, a recently developed

comprehensive wall database (Abdullah, 2019) was utilized, which currently contains detailed information and test results from more than 1100 wall tests surveyed from more than 260 programs reported in literature.

2 Wall Test Database

The main database (Abdullah, 2019) was filtered to obtain a dataset of 71 shear-friction-controlled walls tested under quasi-static, reversed cyclic loading protocols. The dataset includes walls with different cross-section shapes: 58 rectangular, six barbell, five H-shaped, and two L-shaped. Furthermore, the dataset includes walls with different interface conditions at the foundation level or above: cold untreated interfaces (joints), monolithic interfaces, roughened interfaces, and interfaces treated with sealing agents. Similar to the shear-controlled wall dataset, no detailing criteria were applied in filtering to the dataset, because detailing variables such as area of boundary transverse reinforcement (A_{sh}), slenderness ratio of boundary longitudinal bars (s/d_b), and spacing between laterally supported boundary longitudinal bars (h_x) are not typically relevant for shear-friction-controlled walls, i.e., there are no limits placed on these variables in ACI 318-19. The walls in the dataset had shear span ratio (M/Vl_w) ranging between 0.33 to 0.95. Most of the walls in the dataset had no additional applied axial load, whereas for the walls with applied axial load, the axial load did not exceed $0.1A_g f'_c$.

3 Background of Wall Shear-Friction Strength

3.1 Influence of Cyclic Loading on Shear-Friction Strength

The information provided in this subsection is based on content in Paulay et al. (1982). For concrete walls subjected to earthquake cyclic demands imparting relatively large flexural cracking, most of the shear force is transmitted across the flexural compression zone (prior to sliding), as shown in Figure 2(*a*). Once the load reverses, cracks form across the previous flexural compression zone (Figure 2*b*). Until the base moment reaches a level sufficient to yield these bars in compression (close the gap), a wide, continuous crack develops along the foundation-wall interface, and large horizontal shear displacements could occur at this stage of the response. Along this crack, shear is transferred primarily by dowel action of the vertical reinforcement. The wall continues to slide until the compression reinforcement yields, leading to closing of the crack at the compression end of the wall and allowing flexural compression stresses to also be transmitted by the concrete (Figure 2*c*). As a result of the sliding that occurred during this load reversal, the compression in the flexural compression zone is transmitted by uneven bearing across crack surfaces, which reduces both strength and stiffness of the aggregate interlock mechanism along the interface. After a few cycles of reversed loading, sliding displacement can occur along flexural cracks that interconnect and form a continuous, approximately horizontal shear path. At the base of a shear wall, where continuous cracking is likely to be initiated by a construction joint, bending moments also need to be transferred. Consequently, shear transfer along the critical sliding plane is then restricted to the vertical wall reinforcement and flexural compression zone where cyclic opening and closure of cracks will take place. This sliding behavior is quite different than that observed from push-off tests.

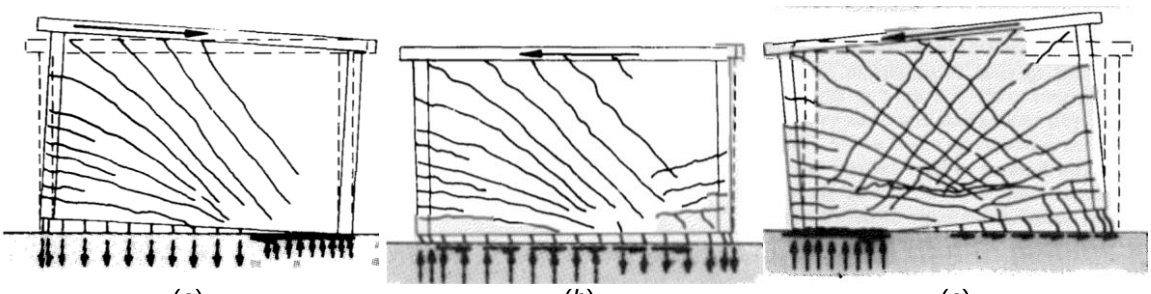

(*a*) (*b*) (*c*)

Figure 2. Development of the sliding shear mechanism (Paulay et al., 1982).

3.2 Influence of Interface Condition on Shear-Friction Strength

Per ACI 318-19, the interface surface condition significantly influences the shear-friction strength. However, the test results reviewed (and discussed later), demonstrate that shear-friction coefficients at concrete interfaces transferring cyclic shear and moment demands are not significantly influenced by the type of the interface. Such interfaces exhibit shear-friction coefficients at the lower end of values specified in ACI 318-19 Section 22.9.4.2. Figure 3(*a*) presents results isolating the role of interface conditions on shear-friction strength and deformation from a series of wall tests with different interface conditions and longitudinal reinforcement layouts.

Test results reported by Anoda (2014) and shown in Figure 3(*a*) indicate that, according to ACI 318-19, wall W1-M is expected to be 2.33 times stronger than walls W1-Js and W2-J. However, test results show that shear-friction strength was similar for a monolithic connection or a cold joint. It is postulated that during the first cycle prior to any sliding occurring, flexural cracks form at a monolithically cast interface, changing the interface from being monolithic to a cracked interface. Figure 3(*a*) also suggests that the longitudinal reinforcement layout in the wall section (uniform distribution vs. concentrated at boundaries) does not have a clear impact on shear friction strength.

Similarly, Figure 3(*b*) shows test results from three identical wall specimens with different interface conditions (Baek et al., 2020), and indicates that walls H0.33OR and H0.33OG with roughened or monolithic interfaces are only about 20% stronger than H0.33OU with an interface that is not intentionally roughened. These tests indicate a coefficient of friction of roughly 0.70 for roughened and monolithic interfaces versus 0.60 for an untreated interface. This modest increase of strength observed for walls H0.33OR and H0.33OG in Figure 3(*b*) is presumably because these walls have smaller aspect ratios than walls in Figure 3(a) (0.33 vs. 0.56), which means less flexural demands and cracking for walls in Figure 3(*b*), resulting in more noticeable effect of interface type. The shorter the aspect ratio of the wall, the closer it is to a push-off test condition shown in Figure 1, which was used to develop the coefficients of friction in ACI 318. Figure 3(*b*) also suggests that failure of roughened and grooved interfaces involves some web crushing at the sliding interface, resulting in reduced ductility.

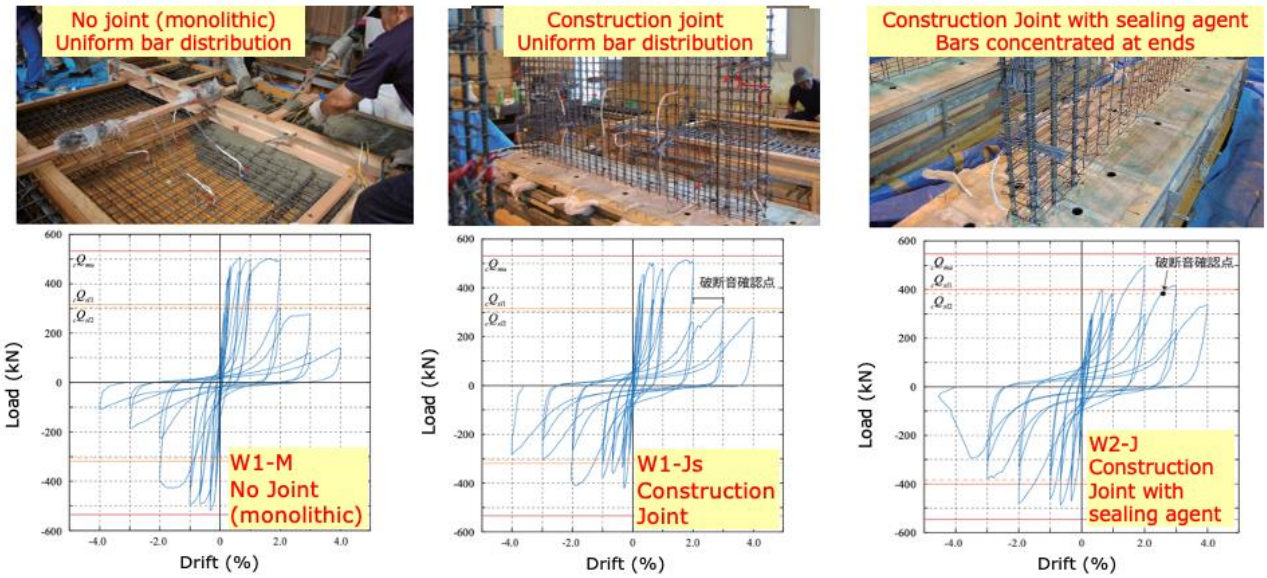

Figure 3. Influence of interface roughness on behavior of shear-friction-controlled walls (Anoda, 2014).

3.3 Influence of Flanges on Shear-Friction Strength

In ACI 318-19, it is not clear whether the longitudinal reinforcement in wall flanges should be consisted in the calculation of shear-friction strength, such that the contribution of longitudinal reinforcement in the flanges is often ignored. However, recent test results suggest that longitudinal bars in wall flanges contribute to shear-friction resistance and should be considered (Kim and Park, 2020; Baek et al., 2020). Figure 4(a) indicates that presence of flanges with vertical reinforcement significantly increases the shear-sliding resistance of walls (40% and 87% increase in the negative and positive directions of loading, respectively). Figure 4(*b*) presents results from three walls with the same web but different cross-section shapes and indicates that longitudinal bars in flanges significantly increase shear-sliding resistance. For the H-shaped wall shown in Figure 4(*b*), it is reported that shear-sliding was limited until diagonal tension cracking through the thickness of the flanges occurred, which was followed by a large slip at the wall-foundation interface; indicating that the flanges restrained shear sliding of the wall web. For the T-shaped wall, when the flange is in tension, sliding resistance is higher partly due to larger compression zone (large neutral axis depth), whereas this effect is not as significant when the flange is in compression (smaller depth of neutral axis).

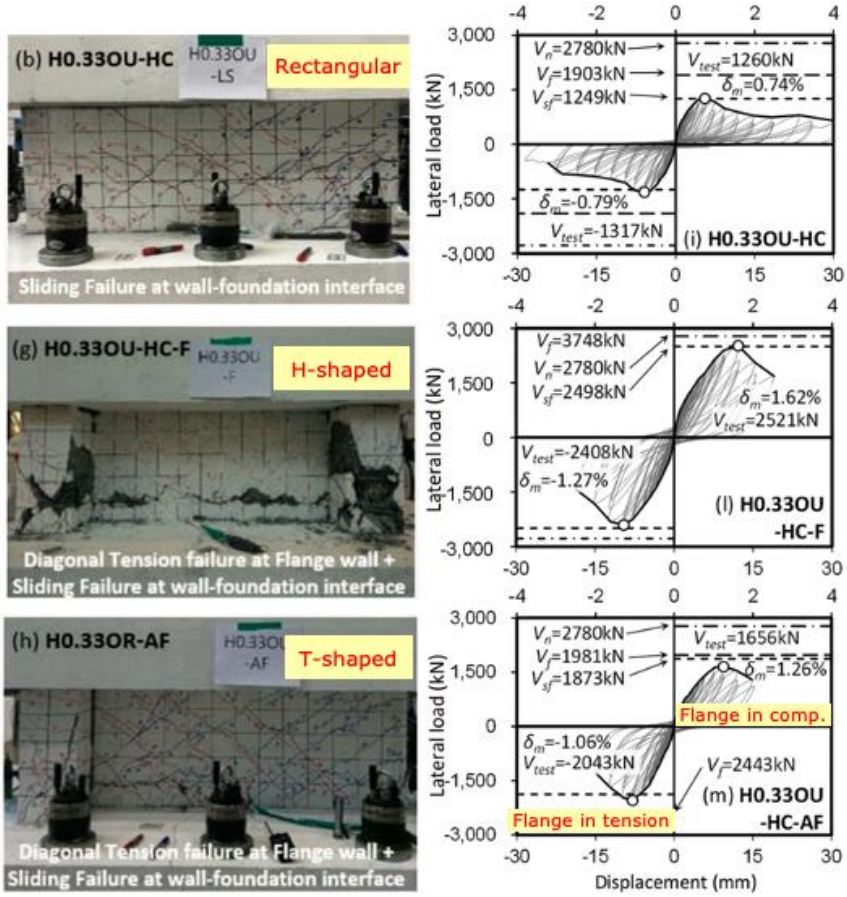

Figure 4. Influence of flanges on behavior of shear-friction-controlled wall tests (Baek et al., 2020).

3.4 Influence of Dowels on Shear-Friction Strength

When shear-friction resistance along an interface is not sufficient to resist shear demands, it is common practice to provide dowels crossing the interface with sufficient development length on both sides of the interface. However, test results (Wasiewicz, 1988; Baek et al., 2018) show that it is possible for the failure plane to shift to the end of the dowel bars, as shown in Figure 5. These results suggest that shear-friction strength should be evaluated at all possible failure planes along the wall or wall segment height, i.e., at the cold joint and at the plane where the dowels end. An appropriate backbone curve to model shear sliding should be located at each potential sliding plane unless the weaker plane can be identified a priori.

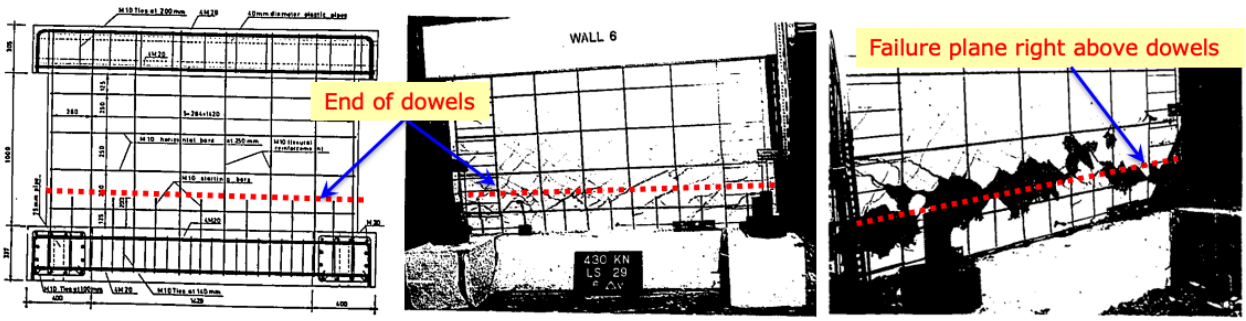

Figure 5. Influence of dowels on changing the location of sliding failure plane (Wasiewicz, 1988).

3.5 Influence of Reinforcement Grade on Shear-Friction Strength

Figure 6 shows results from two identical wall tests with roughened interfaces where reinforcement with different yield strength was used across the interface. Nominal yield strengths, f_y, were 400 MPa (~58 ksi) and 600 MPa (87 ksi). Test results indicate that, for interfaces with both steel grades, the measured shear-friction strength was lower than predicted by ACI 318-19, which is denoted as V_{sf} in the plots. This is results is observed despite ACI 318-19 Table 20.2.2.4(a) limiting yield strength of shear-friction reinforcement to 420 MPa (60 ksi). This limit is apparent in Figure 6 because the shear-friction strengths for the two walls are

identical. Further, test results shown in Figure 7 indicate that, at peak strength, limited yielding of reinforcement crossing the shear friction plane is observed. This result is at odds with the ACI 318-19 assumption (Eq. 1) that all shear-friction bars yield [up to 420 MPa (60 ksi)] when the peak load is reached. Use of higher strength steel for shear friction is permitted by other codes, e.g., Grade 500 MPa (72.5 ksi) in CSA A23.3-04 and KCI 2012, and Grade 600 MPa (87 ksi) in Eurocode 2, Eurocode 8, and fib Model Code 2010.

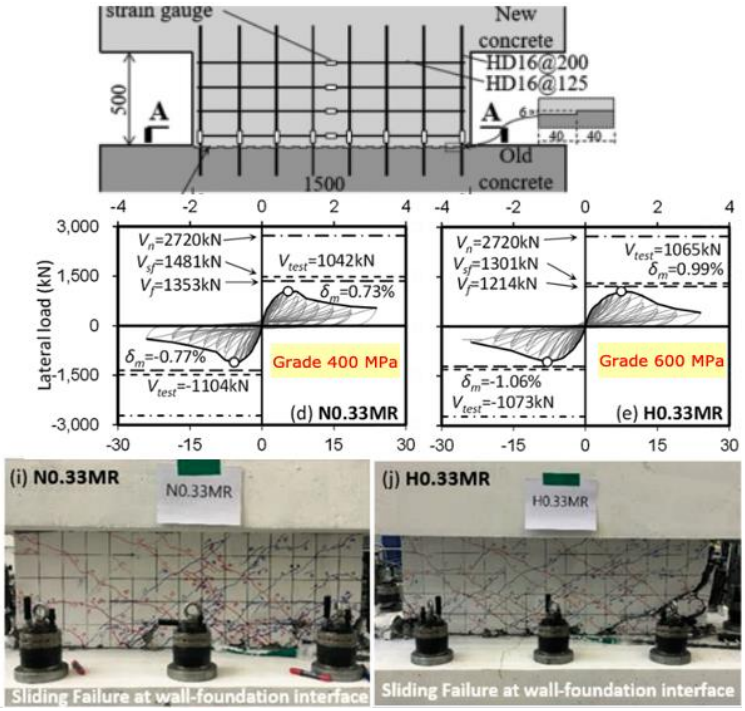

Figure 6. Influence of longitudinal reinforcement yield strength on shear-friction strength (Beak et al., 2020).

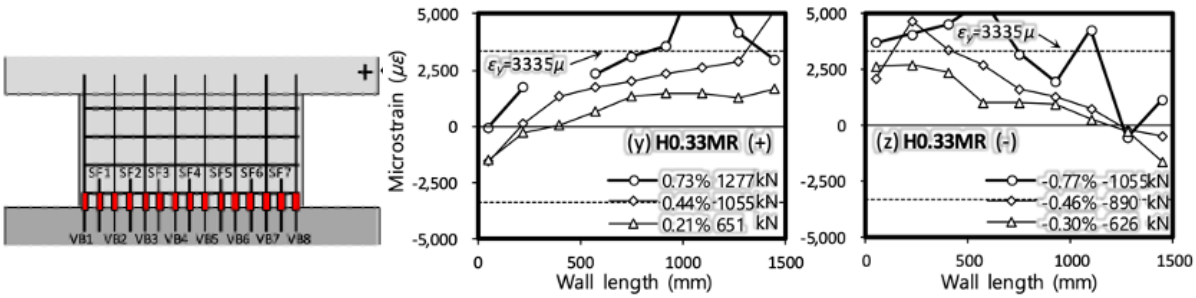

(a) Location of strain gages *(b) Positive loading* *(c) Negative loading*

Figure 7. Measured longitudinal reinforcement strains at wall-foundation interface of a shear-friction-controlled wall test (Beak et al., 2017).

The influence of reinforcement yield strength (steel grade) on shear-friction strength was also investigated using the dataset of 71 wall tests. The results presented in Figure 8 represent measured values of reinforcement yield strength, f_{yE}, which ranges from 300 MPa (40 ksi) to 675 MPa (98 ksi). Results shown in Figure 3-10 present shear-friction strength predictions using the ACI 318-19 shear-friction equation, where $V_{CyfWallSE}$ is determined from Eq. 1 with expected material properties (f'_{cE}, f_{yE}) and without applying the limit on f_{yE} and using μ = 0.6, regardless of the interface type. The figure indicates higher ratios of predicted-to-experimental shear-friction strengths for walls with high strength longitudinal bars ($f_{yE} \geq$ 480 MPa, 70 ksi). This is likely because larger strains are required to reach bar yield, potentially requiring a larger separation at the interface when yield strains are reached. This result suggests that either: (a) a lower μ should be used for higher grades of bars, or (b) reinforcement yield strength should be limited, similar to what is used in ACI 318-19. To address this issue, limiting the expected yield strength of reinforcement (f_{yE}) used for shear-friction resistance to 517 MPa (75 ksi) is proposed. This limit is similar to that used in CSA A23.3-04 and KCI 2012 [i.e., Grade 500 MPa (72.5 ksi)].

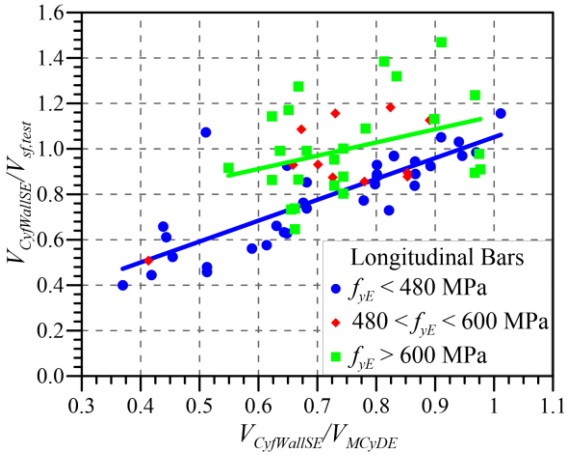

Figure 8. Impact of measured yield strength of longitudinal bars on shear-friction strength (1 MPa = 145 psi).

3.6 Evaluation of ACI 318-19 Provisions

As noted previously, the provisions of ACI 318-19 for shear-friction strength were developed primarily based on results from "push-off" tests under monotonic loading protocols, which differ from wall loading conditions under earthquake demands. Figure 9 compares the measured peak shear friction strength ($V_{sf,test}$) from the-71 wall dataset with the ACI 318-19 limits. As was shown in Table 1, ACI 318-19 includes limits on shear-friction strength. In particular, the 5.5-MPa (800-psi) limit on shear-friction stress for "smooth" cold joints was introduced in ACI 318-71 and has not been revised since. The limited results presented in Figure 9, however, indicate that this 5.5-MPa (800-psi) limit may not be justified by experimental evidence, and thus it is recommended to be removed. Further, Figure 9 suggests that the effect of concrete strength on shear-friction strength is not clear, and that the $0.2f'_{cE}A_{cv}$ limit for untreated (smooth) interfaces seems to reasonably envelope the data (and thus it is retained here).

Figure 10 shows the variation of measured peak shear friction strength ($V_{sf,test}$) from the 71-wall dataset and the ACI 318-19 approach (with assumed μ= 0.6 for all interfaces) versus clamping stress due to longitudinal bars (ρf_{yE}) and axial load (P/A_{cv}). Again, the limited results presented in Figure 10 suggest that the 5.5-MPa (800-psi) upper limit underestimates shear-friction strength significantly for high strength concrete, and that Eq. 1 with μ= 0.6, regardless of the interface type, generally underestimates peak shear-friction strength. The walls with monolithic and roughened interfaces are either on or above the solid line (Eq. 1) in Figure 10, whereas walls with untreated interfaces straddle above and below the solid line, with majority of the data above the line. Moreover, it can be observed from Figure 10 that the type of joint/interface has only a slight-to-moderate influence on peak shear-friction resistance. These results reinforce the earlier observation that the ACI 318-19 values for coefficient of frictions (μ) for roughened and monolithic interfaces over-estimate the shear-friction strength of concrete walls.

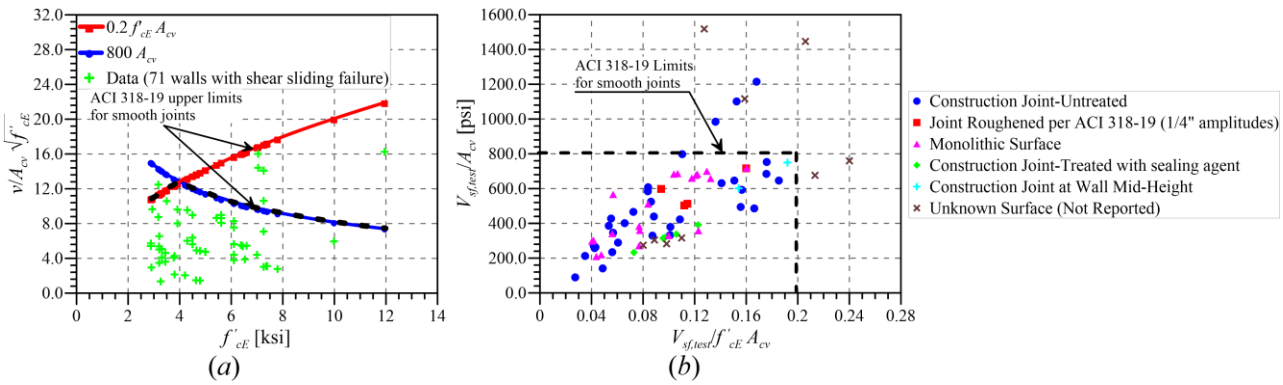

Figure 9. Comparison of measured peak shear friction strength ($V_{sf,test}$) with the ACI 318-19 limits in Table 1.

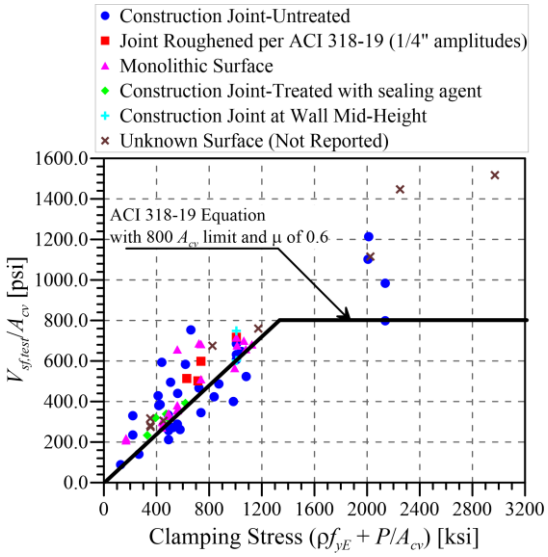

Figure 10. Variation of measured shear friction strength ($V_{sf,test}$) and the ACI 318-19 limits in Table 1 versus clamping stress.

4 Proposed Wall Shear-Friction Strengths

In this section, strength relations for each point on the backbone curve (yield at point B, peak at point C, and residual at point D) are discussed (Figure 11). For each strength, the impact of several variables was investigated; however, only the most relevant variables are discussed here for brevity. It should be noted that the shear-friction strength equations produced are calibrated for walls and wall segments interfaces subjected to reversed cyclic moment and shear. They are not intended for interfaces with differing boundary conditions such as the vertical interface plane between slab and wall.

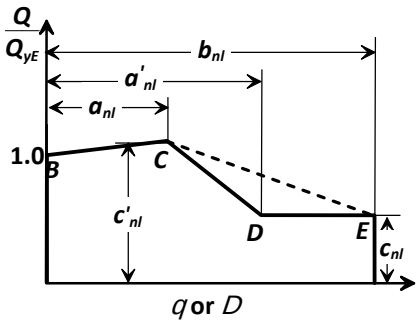

Figure 11. Idealized backbone relations to model translational behavior of shear-friction-controlled walls.

4.1 Yield Strength

Analysis of the 71-wall dataset, indicated that, yield shear-friction strength ($V_{sfy,test}$) is significantly influenced by the wall flexural demand (Figure 8), expressed by either the ratio of shear-friction strength to shear demand at flexural yield ($V_{CyfWallSE}/V_{MCyDE}$), or shear span to length ratio (M/Vl_w), as highlighted in Figure 12. Walls with significant flexural yielding and cracking (i.e., high $V_{CyfWallSE}/V_{MCyDE}$ or M/Vl_w) have lower yield shear-friction strength than walls with limited flexural yielding. Figure 12 also indicates that a modified ACI 318-19 Equation with no upper stress limit and μ = 0.6, results in a mean predicted-to-experimental yield strength ratio of 1.00 and a coefficient of variation of 0.26.

Similarly, to shear- and flexure-controlled walls, the approach taken here was to develop an equation for yield shear-friction strength with a mean of predicted-to-tested values of 1.0 and then apply an amplification factor to obtain peak shear-friction strength.

Based on these results, a new equation is proposed for shear-friction strength at yielding, which corresponds to Point B on the proposed backbone in Figure 11. The expression is given by Eq. 2.

$$V_{CfyWallE} = \left(2.5 - 2.15\frac{V_{CyfWallSE}}{\omega_v V_{MCyDE}}\right) V_{CyfWallSE} \quad \text{Eq. 2}$$

Where $V_{CfyWallE}$ should not be taken greater than 1.8 $V_{CyfWallSE}$ or smaller than 0.8 $V_{CyfWallSE}$.

$$V_{CyfWallSE} = \mu\left(A_{vf} f_{yfE} + N_{UG}\right) \leq 0.2 f'_{cE} A_g \qquad \text{Eq. 3}$$

Where μ is the coefficient of shear friction and is taken as 0.7 for concrete cast monolithically or placed against hardened concrete that is intentionally roughened to a full amplitude of approximately 1/4 in, and 0.6 for concrete placed against hardened concrete that is not intentionally roughened, and N_{UG} is the member gravity axial force. These proposed μ values are based on the discussion provided in Section 3.3.2. Shear-friction strength should be evaluated at all possible failure planes along a wall or wall segment height, such as weak interfaces located at the end of dowel bars, at an existing or potential crack, at an interface between dissimilar materials, or at an interface between two concretes cast at different times. It is possible that a construction joint at the foundation-wall interface with dowel bars (μ = 0.6) is stronger than a monolithic interface (μ = 0.7) at the end of the dowel bars. In Eq 3-2, the expected yield strength of shear friction reinforcement, f_{yfE}, should be reduced if the development length is insufficient to develop f_{yfE} and should not be taken greater than 517 MPa (75 ksi). For flanged wall sections, the reinforcing steel crossing the interface, including the reinforcement within the effective flange width defined in ACI 318-19, should be included in A_{vf}. Eq. 2 and Eq. 3 assume that reinforcement is normal to the interface. For inclined reinforcement, adjustments to the equation should be made as provided in ACI 318-19.

Figure 13 presents results using the yield strength model (Eq. 2) with the experimental data from the dataset and demonstrates that the model matches the experimental data fairly well, with a mean of 1.0 and a coefficient of variation of 0.17.

As a simplified approach to Eq. 2, Eq. 3 can be used. Use of this simplified expression results in increased dispersions (coefficient of variation of ~0.27) compared to Eq. 2.

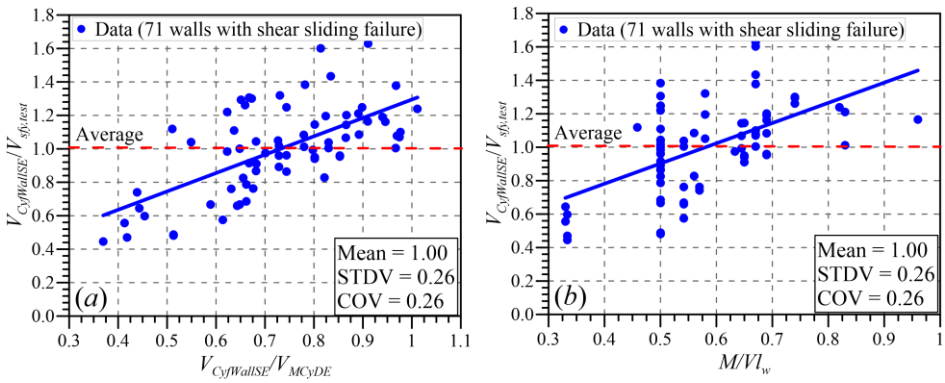

Figure 12. Variation of predicted-to-measured yield shear-friction strength versus shear-friction to flexural strength ratios ($V_{CyfWallSE}/V_{MCyDE}$) and shear span ratios (M/Vlw)

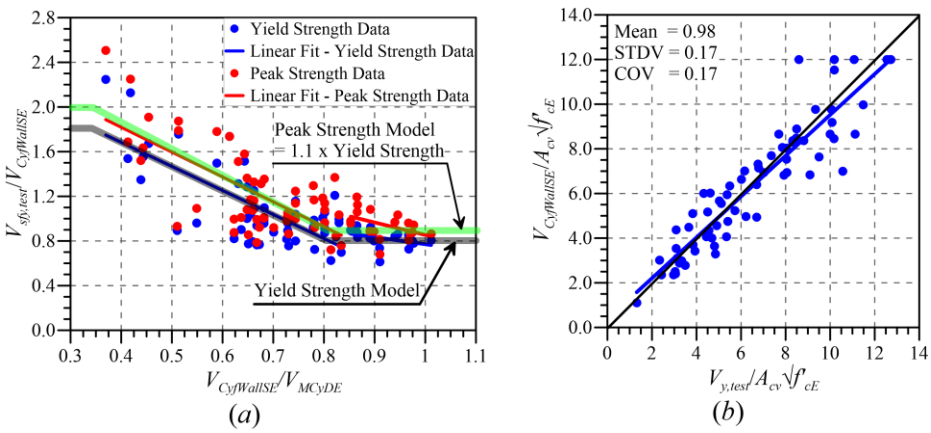

Figure 13. Comparison of estimated and tested yield shear-friction strengths: (a) comparison of model with data, and (b) statistics of the ratio of predicted-to-tested yield strength.

4.2 Peak Strength

Review of the peak strength data in the 71-wall dataset revealed that there is modest hardening from yield to peak strength. Figure 13(a) and Figure 14 show that, on average, peak strength is about 10% higher than yield strength ($V_{sf,peak}$ = 1.10 $V_{CyfWallSE}$). Therefore, it is proposed that peak strength at Point C on the backbone be taken as 1.1 times yield strength at point B, which is the same factor used for shear-controlled walls.

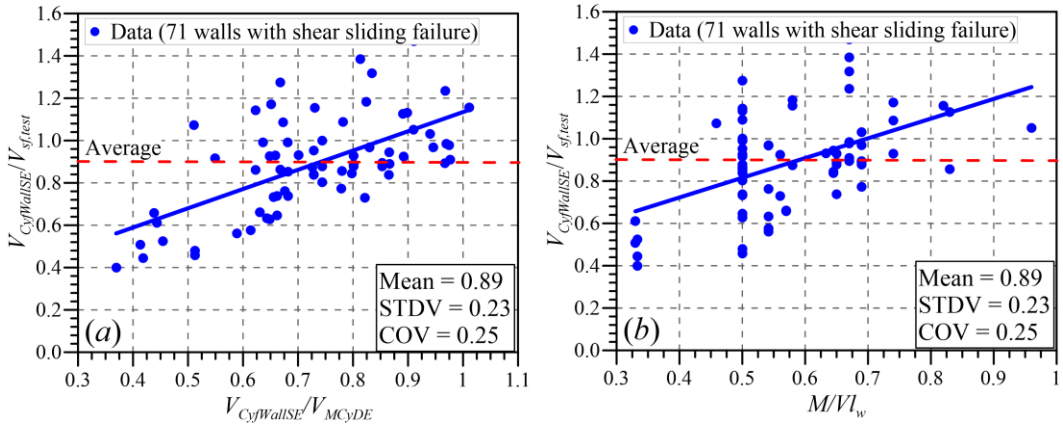

Figure 14. Variation of the ratio of estimated (Eq. 1) to tested shear-friction yield strengths as a function of: (a) $V_{CyfWallSE}/V_{MCyDE}$ and (b) M/Vl_w.

4.3 Residual Strength

Generally, shear-friction-controlled walls have larger residual strength than flexure- or shear-controlled walls. On average, the residual strength of the wall tests in the 71-wall dataset is roughly 0.6 of their yield strength, as shown in Figure 15. Figure 15(*a*) shows a slight correlation of residual strength with $V_{CyfWallSE}/V_{MCyDE}$, whereas Figure 15(*b*) shows that there is a significant correlation of residual strength with clamping stress and type of interface. For roughened and monolithic interfaces, the residual strength is lower because, as was noted from Figure 3(*b*), failure of roughened and grooved/monolithic interfaces involves moderate to significant concrete crushing at the sliding interface, depending on the level of clamping force on the interface, leading to faster degradation of strength once lateral strength loss initiates. Given the uncertainly and dispersion in the data, it is proposed to take the residual strength as 0.5 and 0.6 of yield strength for monolithic/roughened and untreated interfaces, respectively.

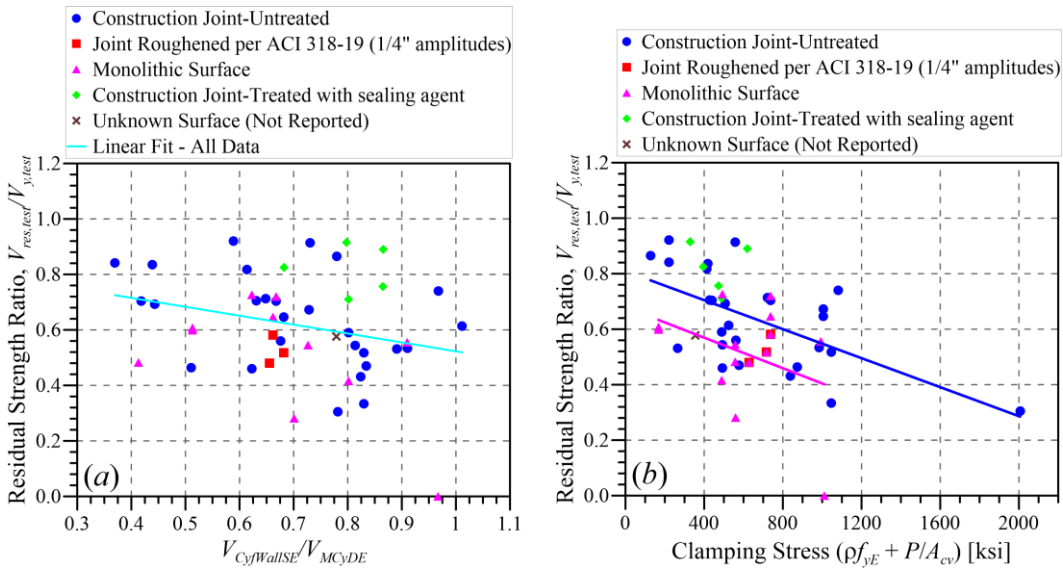

Figure 15. Variation of measured residual strength to yield strength as function of: (a) $V_{CyfWallSE}/V_{MCyDE}$ and (b) clamping stress.

5 Conclusions

This study involves utilizing available experimental data from 71 wall tests and new information on performance of structural walls to develop MPs and AC for seismic evaluation and retrofit of shear-friction-controlled reinforced concrete walls. Based on the results, the following conclusions are reached:

1. The ACI 318-19 approach for shear-friction strength developed from "push-off" tests under primarily monotonic loading, does not capture the shear-friction strength at interfaces undergoing inelastic cyclic loading. Under cyclic loading, the contributions of direct bearing of asperities and reinforcement dowel action are both reduced.
2. The ACI 318-19 coefficients of friction (μ) for roughened and monolithic interfaces tend to over-predict the shear-friction strength for concrete wall interfaces subjected to cyclic loading. The interface surface condition does not influence shear-friction strength as significantly as implied by ACI 318-19, possibly because the cyclic moment and shear loading opens interface cracks and weakens the transfer mechanism reducing the coefficient of friction to the lower values in ACI 318-19, regardless of interface treatment. Cycled interfaces exhibit shear-friction coefficients on the lower end of values given in ACI 318-19, with μ = 0.7 or 0.6 for roughened/monolithic and untreated interfaces, respectively.
3. Shear-friction yield strength relations are proposed that modify the ACI 318-19 shear-friction equation with reduced friction coefficients and introducing the effects of the ratio of shear-friction strength to shear demand at flexural yielding ($V_{CyfWallSE}/V_{MCyDE}$). Interfaces with larger flexural demands are given reduced shear-friction strength.
4. Despite the proposed low coefficients of friction for interfaces sustaining cyclic loading, interfaces with relatively low moment demands can see their shear friction strengths increase beyond values provided by ACI 318-19.
5. Longitudinal bars in flanges are found to contribute to shear-friction resistance and should be considered in the calculation of shear-friction strength.
6. At peak strength, limited reinforcement yielding occurs in the web, regardless of the reinforcement grade. For high strength bars, a larger separation at the interface is needed for the bars to reach yield and to mobilize the full bar yield strength. Thus, it is proposed that the useable yield strength of reinforcement resisting shear-friction be limited to 517 MPa (75 ksi).
7. Test results indicate that it is possible for the shear-sliding failure plane to shift to the end of wall dowel bars, where the steel area is reduced, and monolithic concrete conditions exist.
8. ACI 318-19 includes limits on friction strength, which are mostly due to lack of experimental data. In particular, the 5.5-MPa (800-psi) limit for "smooth" cold interfaces was introduced in the ACI 318-71 edition and has not been revised since. Results presented indicate that this limit may not be justified by experimental evidence, and thus it is recommended to be removed. The results also revealed that the effect of concrete strength on shear-friction strength is not clear, and that the $0.2f'_c A_{cv}$ limit for untreated (smooth) interfaces seems to well envelope the data, and thus it is recommended to be retained.
9. Review of the peak strength data in the database revealed that there is roughly 10% hardening from yield strength to peak strength.

6 Acknowledgements

Funding for this study was provided, in part, by FEMA through ATC-140 Project, and the University of California, Los Angeles. The author would also like to thank the Project Technical Committee for providing thoughtful comments on the work presented. Any opinions, findings, and conclusions or recommendations expressed in this paper are those of the authors and do not necessarily reflect the views of others mentioned here.

7 References

Abdullah, S. A. (2019). *Reinforced concrete structural walls: Test database and modeling parameters*, Ph.D. dissertation, University of California, Los Angeles, California.

ACI (2019). Building code requirements for structural concrete (ACI 318-19). American Concrete Institute, Farmington Hills, MI.

ACI (1971). *Building code requirements for reinforced concrete (ACI 3 18-71)*, American Concrete Institute, Farmington Hills, MI.

ACI (2017). *Standard requirements for seismic evaluation and retrofit of existing concrete buildings (ACI 369.1-17) and commentary*, American Concrete Institute, Farmington Hills, MI.

Anoda, J. (2014). *Effect of construction interface and arrangement of vertical bars on slip behavior of shear walls*, Master's Thesis, Nagoya Institute of Technology, Nagoya, Japan. (in Japanese)

ASCE (2017). *Seismic evaluation and retrofit of existing buildings (ASCE/SEI 41-17)*, American Society of Civil Engineers, Reston, VA.

Baek, J.W., Park, H.G., Lee, B.S., Shin, H. M. (2018). Shear-friction strength of low-rise walls with 550 MPa (80 ksi) reinforcing bars under cyclic loading, ACI Structural Journal, V. 115, No. 1, pp. 65-78.

Baek, J., Kim, S., Park, H., Lee, B., (2020). Shear-friction strength of low-rise walls with 600 MPa reinforcing bars, ACI Structural Journal, 17(1): 169-182.

Birkeland, P. W., Birkeland, H. W. (1966). Connections in precast concrete construction, ACI Journal Proceedings, 63(3): 345-368.

British Standards Institution (2004*). Eurocode 2: Design of Concrete Structures - Part 1-1: General Rules and Rules for Building, European Standard EN-1992-1-1:2004: E*, European Committee for Standardization, Brussels, Belgium.

British Standards Institution (2003). *Eurocode 8: Design of structures for earthquake resistance*, European Committee for Standardization, Brussels, Belgium.

CSA (2004). *Design of Concrete Structures*, Canadian Standards Association, Rexdale, Ontario, Canada.

Elwood, K. J., Matamoros, A. B., Wallace, J. W., Lehman, D. E., Heintz, J. A., Mitchell, A. D., Moore, M. A., Valley, M. T., Lowes, L. N., Comartin, C. D., Moehle, J. P., (2007) Update to ASCE/SEI 41 Concrete Provisions, Earthquake Spectra, 23(3): 493-523.

FEMA (1997a). *NEHRP Commentary on the guidelines for the seismic rehabilitation of buildings (FEMA-274)*, Federal Emergency Management Agency, Washington, DC.

FEMA (1997b). *NEHRP Guidelines for the seismic rehabilitation of buildings (FEMA-273)*, Federal Emergency Management Agency, Washington, DC, 435.

Hofbeck, J. A., Ibrahim, I. O., Mattock, A.H., (1969). Shear transfer in reinforced concrete, Journal of the American Concrete Institute, 66(2): 119-128.

FIB (2013). *fib Model Code for Concrete Structures 2010*, International Federation for Structural Concrete, Wilhelm Ernst & Sohn, Berlin, German.

Kahn, L. F., Mitchell, A. D., (2002). Shear friction tests with high strength concrete, ACI Structural Journal 99 (1): 98-103.

Kim, J.H., Park, G.P., (2020). Shear and shear-friction strengths of squat walls with flanges, ACI Structural Journal, 117(6): 269-280.

KCI (2012). *Concrete design code and commentary*, Korea Concrete Institute, Kimoondang, Korea.

Mattock, A. H. (1976). Shear Transfer under Monotonic Loading Across an Interface Between Concretes Cast at Different Times, University of Washington, Report SM 76-3, Seattle, WA.

Mattock, A. H. (1977). Considerations for the design of precast concrete bearing wall buildings to withstand abnormal loads, PCI Journal, 22 (3): 105-106.

Paulay, T., Priestley, M.J.N., Paulay, T., (1982). Ductility in earthquake resisting squat shear walls, ACI Structural Journal, 79(4): 257-269.

Wasiewicz, Z., (1988). *Sliding shear in low rise shear walls under lateral load reversals*, Master Dissertation, University of Ottawa, Canada.

Wiradinata, S., (1985). *Behavior of squat walls subjected to load reversals*, Master's Thesis, University of Toronto, Toronto, Canada.